Criteria for the assessment of the influence of atmospheric turbulence on wind turbine noise propagation

Bill Kayser, David Écotière, Benoit Gauvreau

Acta Acustica 2023, **7**, 63

https://doi.org/10.1051/aacus/2023051

Available online at:
https://acta-acustica.edpsciences.org

SCIENTIFIC ARTICLE OPEN ACCESS

Criteria for the assessment of the influence of atmospheric turbulence on wind turbine noise propagation

Bill Kayser[1,*], David Écotière[1], and Benoit Gauvreau[2]

[1] UMRAE, Cerema, Université Gustave Eiffel, 11 rue Jean Mentelin, BP 9, Strasbourg 67035, France
[2] UMRAE, Université Gustave Eiffel, Cerema, Allée des Ponts et Chaussée Route de la Bouaye, Bouguenais 44340, France

Received 24 May 2022, Accepted 21 September 2023

Abstract – This paper investigates the influence of atmospheric turbulence on the propagation of wind turbine noise using an aeroacoustic source model coupled with a parabolic equation propagation model. Sets of simulations with and without atmospheric turbulence are performed, allowing the determination of a simple formulation that quantifies the uncertainties of the A-weighted sound pressure level (SPL) when the modelling does not account for atmospheric turbulence. For the case study, the results show that atmospheric turbulence has a negligible effect on SPL up to 800 m from the wind turbine, even under upwind conditions. While the conclusions are specific to this case study, the method appears promising for simplifying the calculation of atmospheric turbulence effect in wind turbine noise studies. A freely accessible online application has been developed to present additional results.

Keywords: Wind turbine noise, Atmospheric turbulence

1 Introduction

Residents living near wind farms sometimes report annoyance caused by wind turbine noise. These situations can lead to the implementation of degraded operating modes (acoustic curtailments), which induce a loss of energy production. It is thus imperative to develop reliable methods for predicting wind turbine noise in outdoor environments.

It is now well-known that accurate modelling of wind turbine noise requires considering the wind turbine as an extended sound source [1, 2], whose main noise generation mechanism is related to aeroacoustic phenomena [3–5]. The influence of outdoor sound propagation effects must also be considered, as they lead to non-negligible variability on Sound Pressure Level (SPL) at long range from the source [6–9].

Among the meteorological effects, turbulent eddies in atmosphere can influence outdoor sound propagation. This influence is known to be predominant on SPL under upwind propagation situations when considering a point source close to the ground. However, little information is available for extended and elevated sound sources, such as wind turbines. Furthermore, existing numerical propagation methods that can take into account atmospheric turbulence are generally very time-consuming compared to methods for a non-turbulent atmosphere. The purpose of this paper is to investigate the feasibility of determining simple formulations to account for the effect of atmospheric turbulence on SPL predictions.

Firstly, we determine receiver locations (distance and angle from wind direction) for which turbulence effects are negligible. Secondly, we estimate bias and uncertainties in the areas where turbulence is not negligible. Finally, we propose new formulations to adjust the A weighted SPL predictions if using a propagation model that do not explicitly take into account atmospheirc turbulence effects.

The paper is organized as follows: Section 2 presents the modelling that considers the dominant broadband aerodynamic noise mechanism involved in wind turbine noise emission, as well as propagative effects such as wave refraction, atmospheric absorption, atmospheric scattering and ground effects. Section 3 presents simulations for a turbulent atmosphere compared to simulations for a non-turbulent atmosphere, in order to provide quantitative and practical results. Section 4 presents conclusions and discusses the perspectives.

2 Wind turbine noise modelling

2.1 Moving monopoles approach

The moving monopoles approach, developed by [10], is used to model wind turbine noise. A strip theory is employed, consisting of splitting each blade into segments of variable chord and span, in order to consider a non-uniform incidence flow along the blades. The angle-dependent

*Corresponding author: bill.kayser@cerema.fr

sound power level of each segment is obtained using Amiet's theory, as detailed in [4].

An attenuation term is then calculated using a propagation model based on the wide-angle parabolic equation (WAPE) approximation of the wave equation [11]. This allows us to take into account the propagative effects that occur between the wind turbine and far-field receivers. The summation of contributions from all blade segments is then performed at the receivers, assuming that all the contributions are uncorrelated [12].

The wind turbine considered here has a nominal electrical power of 2.3 MW, a rotor diameter of 93 m, a hub height of 80 m, and three blades of 45 m in length. The speed of rotation measured at the hub height increases linearly from 6 rpm at the cut-in wind speed of 4 $m \cdot s^{-1}$ to 16 rpm at a wind speed of 12 $m \cdot s^{-1}$. Since the wind turbine noise limits are related to the highest noise imission at the receiver, this study is performed for wind speed of 12 m/s at hub height. The reader may refer to [13, 14] for more complete details about the wind turbine noise modelling.

2.2 Sound waves refraction

The modelling assumes an inhomogeneous propagation medium, where the real moving atmosphere is considered as a hypothetical motionless medium with the effective sound speed $c_{\text{eff}} = c + u_x$, where u_x is the wind velocity component along the direction of sound propagation, and c is the sound speed in the air. The average vertical profile of effective celerity is defined as follows:

$$\langle c_{\text{eff}}(z)\rangle = \sqrt{\gamma R T_0} + \langle U(z)\rangle \cos\theta, \tag{1}$$

where $\gamma = 1.4$ is the heat capacity ratio of air, $R = 8.31$ J $\cdot$ mol^{-1} $\cdot$ K^{-1} is the perfect gas constant, $T_0 = 10$ °C is the air temperature chosen here to be representative of an average scenario, θ is the angle between the wind direction and the sound propagation direction which ranges from 0° to 180° because of the symmetry of the problem according to the wind direction, $\langle U(z)\rangle$ is the mean vertical wind speed profile. We assume that the mean vertical wind profile is logarithmically shaped [15]:

$$\langle U(z)\rangle = a_u \ln\left(\frac{z}{z_0}\right), \tag{2}$$

where $a_u = 1.67$ $m \cdot s^{-1}$ accounts for a strong mean refraction coefficient due to the influence of wind [16], and $z_0 = 0.01$ m is the roughness height of the wind profile.

2.3 Atmospheric absorption

The atmospheric absorption is taken into account following the standard [17]. It depends on the air temperature T_0 (K), the atmospheric pressure patm (Pa) and the relative humidity of air h_r (%) set to 80%.

2.4 Atmospheric turbulence scattering

Under upwind conditions, acoustic energy is scattered into the shadow zone due to atmospheric turbulence. The strength of this scattering depends on turbulence parameters, as well as the acoustic frequency and geometry [18, 19]. To accurately predict SPL in these conditions, simulations are performed using a WAPE model, which explicitly models the influence of atmospheric turbulence on SPL [20].

The turbulence is generated using a Random Fourier Mode technique, which produces random realizations (50 in this work) of the turbulent index to obtain an average value for the overall SPL estimation. This approach is based on the hypothesis of a "frozen medium", as it assumes that sound waves travel so fast that the medium can be considered frozen ([21], p. 205). The refractive index $n = \langle n\rangle + \mu$ is thus perturbed, where $\langle n\rangle$ accounts for refraction effects, while the stochastic part μ accounts for turbulence effects.

In this work, the turbulent energy spectrum considered is a von Kármán spectrum [22, 23], with turbulence scales L ranging from 0.01 m to 1.1 m, and $\mu^2 = 10^{-5}$. These typical values have been reported in the literature [20, 24–26]. It is important to bear in consideration that distinct values of these parameters may yield different results. Furthermore, note that this approach is based on a scalar representation of turbulence's effect on SPL modelling. Some studies have suggested considering atmospheric turbulence using anisotropic and heterogeneous models [26, 27]. While these atmospheric turbulence models offer a more precise formulation of the physical phenomena, this paper make the hypothesis that considering isotropic and homogeneous turbulence is sufficiently accurate within the scope of this operational study, particularly when focusing on overall A-weighted SPL that are averaged over one blade rotation (see Sect. 3).

2.5 Ground effects

The ground influence on sound propagation is taken into account using the Miki's impedance model [28] that depends on the airflow resistivity parameter σ. We consider $\sigma = 1000$ Kn $\cdot$ s $\cdot$ m^{-4} (e.g., compacted ground) as it is representative of ground usually encountered around wind turbines. The frequency range is $f \in [50; 1000]$ Hz, that is the range for which the acoustic emission is the most significant for wind turbine noise [29]. The frequency validity of Miki's model is thus satisfied: $0.01 < \frac{f}{\sigma} < 1$ [30], where $\rho_0 = 1.24$ kg $\cdot$ m^{-3} is the density of air.

3 Results

3.1 Methodology

The turbulence effect is evaluated by comparing wind turbine noise modelling without atmospheric scattering (i.e., $\mu^2 = 0$), resulting in drastically low SPL in the shadow zone, to wind turbine noise modelling with atmospheric scattering caused by a strong turbulence factor (i.e., $\mu^2 = 10^{-5}$) [24, 25]. In the latter case, the sound propagates into the shadow zone and interference dips. The difference in sound levels between the two scenarios is referred to as the "bias" and can be considered as an "insertion loss" term. The study considers several propagation angles θ ranging

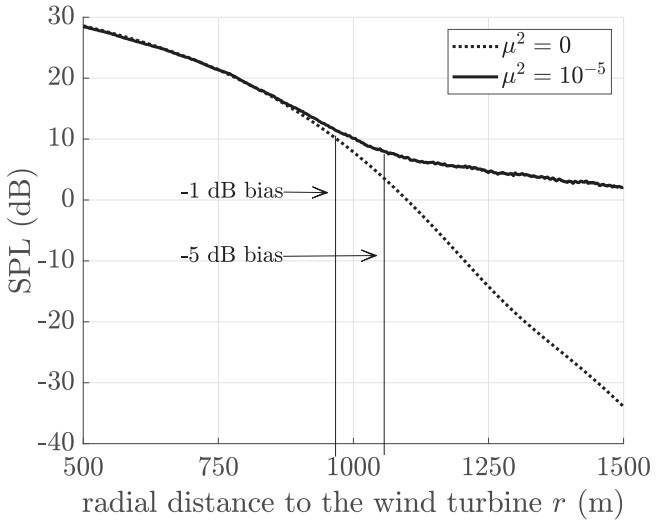

Figure 1. Example of wind turbine noise modelling when the wind turbine operates at its maximum rpm, for $f = 100$ Hz, $\theta = 180°$, receivers height $z_r = 2$ m, and distance $r \in [500; 1500]$ m. The turbulence effect is estimated *via* a bias term corresponding to the difference of the scenario without turbulence ($\mu^2 = 0$) and the scenario with turbulence ($\mu^2 = 10^{-5}$).

from 0° (downwind) to 180° (upwind) in increments of 20°, and calculations are performed for the center frequencies of each one-third octave band within the range $f \in [50; 1000]$ Hz. As an example, the Figure 1 illustrates the methodology for $f = 100$ Hz, $\theta = 180°$, and a receiver height $z_r = 2$ m.

3.2 Monochromatic analysis

Figure 2 presents isolines of bias for all center frequencies considered, where $\theta \in [0; 180]°$ and $r \in [500; 1500]$ m, a receiver height $z_r = 2$ m and a bias of -5 dB. Two areas can be identified:

- The isolines represent the shadow zone boundaries induced by upwind refraction. A typical behavior is observed where the refraction impacts all the third octave bands SPL, but where the shadow zone boundary differs between frequencies. The boundary appears at longer distance for low frequencies (≈1400 m for $f = 50$ Hz) than for high frequencies (≈800 m for $f = 1000$ Hz), which is due to the different wavelengths. One can also notice that the shadow zone appears at shorter range when θ tends to 180°, which is the strongest upwind refraction condition.
- The isolines account for destructive interference patterns that are due to ground effects. These interference patterns occur at some specific frequencies (250 Hz, 315 Hz, 800 Hz, and 1000 Hz) and at some specific distances from the source because they are linked to the geometry of the case study, i.e., source height, receivers location and relative sound wavelength. These interference patterns are visible on Figure 2 because turbulence scatters sound wave in these destructive interference regions, leading to an SPL variability greater than the chosen bias of -5 dB.

It is important to note that the isolines represented on Figure 2 are valid for the case study presented at a receiver height $z_r = 2$ m. We verified that a similar behavior is observed for other receiver height within $z_r \in [0.5; 3]$ m.

3.3 Estimation of the shadow zone boundary for various bias values

This section investigates the influence of atmospheric turbulence on overall A-weighted SPL predictions. We compute the A-weighted SPL using monochromatic calculations at the center frequencies f of one-third octave bands with $f \in [50; 1000]$ Hz. Figure 3 illustrates the 2D polar map (θ, r) of the bias, which enables the visualization of locations where atmospheric turbulence significantly affects SPL predictions (see Fig. 3 where the shadow zones are represented on the left side of each boundary).

Figure 3 shows that the maximum bias are located in the shadow zone, i.e., for strong upwind conditions ($\theta > 120°$) and far from the source ($r > 800$ m). The isolines in Figure 3 represent the boundary distance of the shadow zone from the wind turbine, considering various threshold bias assumptions. These curves can be accurately fitted ($R^2 = 0.999$, $p_{\text{value}} < 2.2\text{e-}16$) using a hyperbolic equation, yielding a simple expression for the distance of the shadow zone from the wind turbine:

$$d_{\text{shadow}}(\theta) = \frac{p}{1 - e\cos\left(\theta\frac{\pi}{180}\right)}. \tag{3}$$

The parameters e and p are given in Table 1 for several bias values. They are valid only for the case study considered here: wind turbine dimension, ground properties etc.

The distance calculated with equation (3) allows us to consider three cases for assessing the influence of turbulence:

- For crosswind and downwind situations ($\theta < 110$), the bias is positive and quite low (bias: mean 0.4 dBA, standard deviation 0.1 dBA, see Fig. 4), which means that turbulence effect decreases SPL in this area. This is because turbulence scatters sound waves from high to low SPL locations, and smooth interference patterns due to ground effects.
- For downwind conditions, outside the shadow zone ($r < d_{\text{shadow}}$ ($\theta > 110$)) the bias is similar to that for crosswind and downwind situations and indicates a negligible effect of turbulence (mean bias of 0.4 dBA, see Fig. 4).
- For downwind conditions, inside the shadow zone ($r < d_{\text{shadow}}$ ($\theta > 110°$)), the bias is negative and not negligible. We observe an increase of the SPL due to the scattering of sound from the outside of the shadow zone to the inside. The bias increases with the distance and the angle, where the maximum bias is observed for maximum upwind angle (180°) reaching -27 dBA at 1500 m.

3.4 Bias estimation relative to the distance from the wind turbine

It is also possible to use a wind turbine noise model that do not take into account atmospheric turbulence effect,

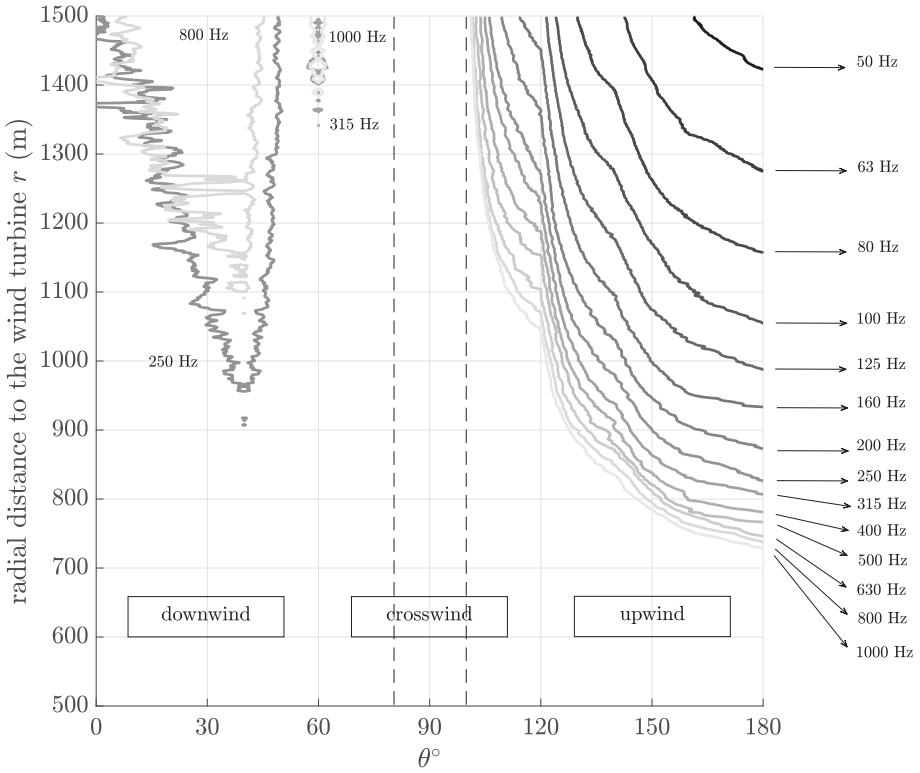

Figure 2. Isolines corresponding to a −5 dB bias between modelling without atmospheric turbulence ($\mu^2 = 0$) and with high atmospheric turbulence ($\mu^2 = 10^{-5}$) at $z_r = 2$ m. Each isoline represents a center frequency f of the one-third octave bands for $f \in [50; 1000]$ Hz. The results are plotted in the 2D space (θ, r) where θ is the propagation angle and r the distance to the wind turbine.

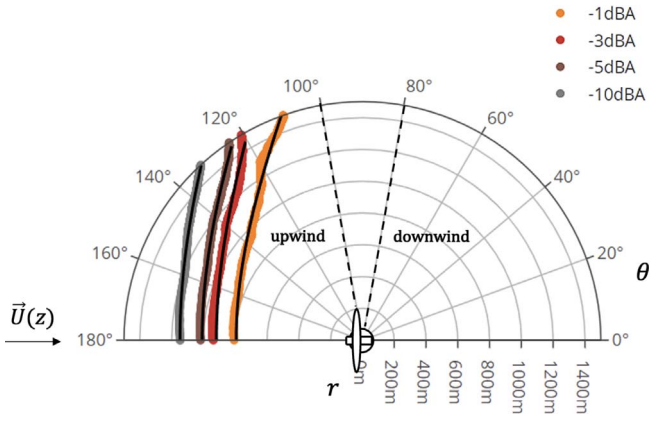

Figure 3. Isolines corresponding to bias of −1, −3, −5, −10 dB between modelling without atmospheric turbulence ($\mu^2 = 0$) and with high atmospheric turbulence ($\mu^2 = 10^{-5}$) at $z_r = 2$ m, for overall A SPL. The results are plotted in polar coordinates with θ the propagation angle, r the distance to the wind turbine, and $\vec{U}(z)$ the wind vector. The black lines correspond to fitting curves calculated with equation (3).

provided that an uncertainty term is associated with this choice. The 95% confidence interval of SPL including turbulence effect is given by L_{PA}, with:

$$L_{\mathrm{PA}} \in [L_{\mathrm{PA,noturb}} - b - k\,u_b; L_{\mathrm{PA,noturb}} - b + k\,u_b], \quad (4)$$

where $L_{\mathrm{PA,noturb}}$ is the A-weighted SPL prediction without modelling the turbulence effect, and L_{PA} is the A-weighted SPL that takes into account the turbulence effect. Let b be the bias (mean error), u_b the standard uncertainty associated with the bias, and k a coverage factor to get the 95% confidence interval (see below). The bias, that depends on the distance and on the propagation angle, can be estimated for several propagation angles with a polynomial regression on the distance to the wind turbine (see Fig. 5):

$$b(\theta) = b_0(\theta) + b_1(\theta)r + b_2(\theta)r^2. \quad (5)$$

The standard deviation u_b is estimated by calculating the standard deviation of the residuals of the polynomial regression. Assuming a Gaussian distribution of residuals, the coverage factor $k = 2$ is considered here to estimate the width of the 95% confidence interval. Examples of values of b_0, b_1, and b_2 are given in Table 2.

4 Discussion and conclusion

This paper investigates the impact of turbulence on wind turbine noise propagation predictions in a scenario that maximizes propagation effects (representing the most challenging case for residents). It explores the possibility of using a propagation model that does not explicitly consider turbulence effects to accurately predict A-weighted SPL.

This study finds that the influence of atmospheric turbulence on A-weighted SPL predictions is negligible (with

Table 1. Parameters values for p and e, according to the different bias considered. The coefficient of determination R^2 and the p_{value} are also presented.

Bias (dBA)	p	e	R^2	p_{value}
−1	2780	2.50	0.999	$<10^{-16}$
−3	3580	2.90	0.999	$<10^{-16}$
−5	3530	2.50	0.999	$<10^{-16}$
−10	4130	2.60	0.999	$<10^{-16}$

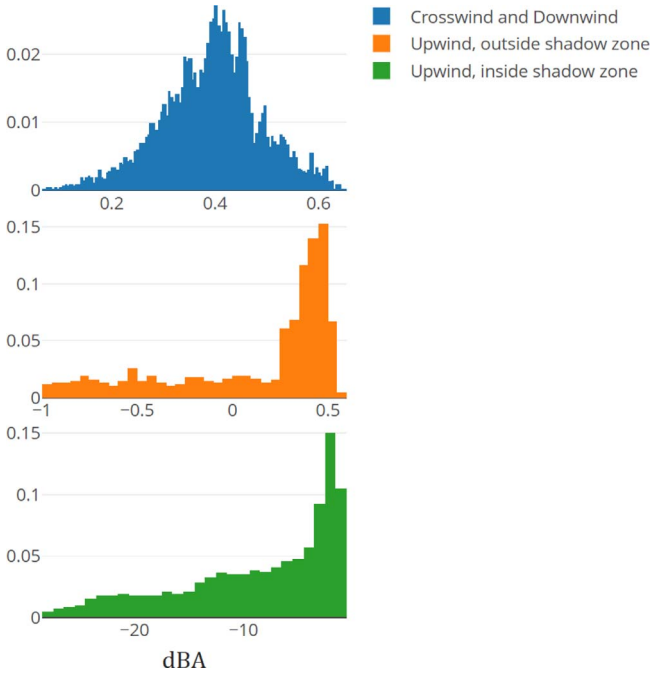

Figure 4. Bias distributions for overall A-weighted SPL predictions for crosswind and downwind conditions (top), upwind conditions outside the shadow zone (middle) and upwind conditions inside the shadow zone (bottom).

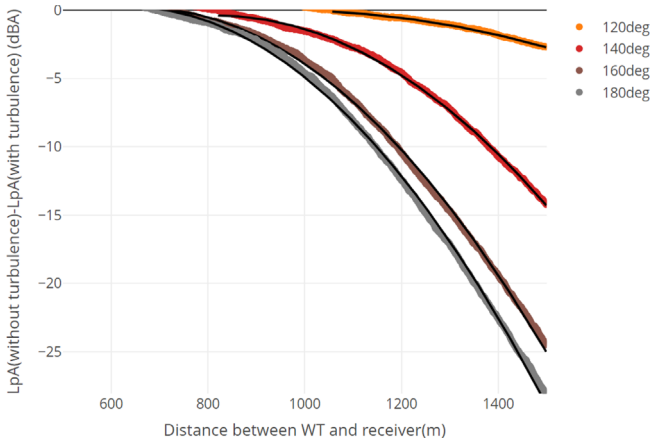

Figure 5. Bias inside the shadow zone represented for several propagation angle θ. The black lines correspond to fitted curves according to equation (5).

Table 2. Coefficients of the polynomial model for the bias. R^2 and p_{value} are respectively the squared correlation coefficient and the probability value of the polynomial regression. The term u_b is the standard uncertainty associated with the bias estimation.

θ	b_0 (θ)	b_1 (θ)	b_2 (θ)	R^2	u_b (θ) (dBA)
180°	−14.9	2.72×10^{-2}	-1.27×10^{-52}	0.997	<0.1
160°	−25.3	5.69×10^{-2}	-3.31×10^{-5}	0.999	0.1
140°	−12.3	4.21×10^{-2}	-3.37×10^{-5}	0.999	0.2
120°	−12.0	4.37×10^{-2}	3.65×10^{-5}	0.999	0.2

an absolute bias value of <0.5 dBA) for distances up to 800 m in all propagation directions (downwind and upwind) and up to 1000 m for a propagation direction of −120° to 120°. Consequently, using a wind turbine noise propagation model that accounts for turbulence is unnecessary in these cases, even under upwind conditions. Corrections for A-weighted SPL can be made with a small bias, typically around 0.5 dBA (mean bias 0.4 dBA, standard deviation of bias 0.1 dBA, for the standard case studied here). The influence of turbulence becomes significant for propagation angles $120° > \theta > 180°$, where the shadow zone boundary is approximately 1000 m for $\theta = 120°$ and 800 m for $\theta = 180°$ due to sound scattering in these regions.

This study also provides guidance on how to estimate a confidence interval for A-weighted SPL, accounting for turbulence effects in the shadow zone, using A-weighted SPL predicted by a propagation model that does not explicitly consider turbulence's influence on sound propagation. Additional calculations can be performed using an online application [31].

It is important to note that the specific parameter values given for estimations of d_{shadow} (Fig. 3) for A-weighted SPL are based on specific assumptions for the studied case, such as natural ground, high wind speed, 2 m high receiver, 80 m hub height, etc. However, other choices of input parameters do not significantly change the presented results. For example, variations in receiver heights from 1.5 m to 3 m yield very similar trends and conclusions (see online *Shiny* application for testing other values [31]).

Nonetheless, it is acknowledged that different choices of wind speed assumptions may lead to different results. The chosen approach was to maximize sound emission and turbulence effects on sound propagation, representing a most challenging case and a worst case for inhabitants. Lower wind speeds might result in less significant effects of atmospheric turbulence on sound propagation, leading to a shadow zone that is farther away. The study does not account for wake effects, which could influence sound propagation in downwind situations [32, 33]. Additionally, the anisotropic aspect of atmospheric turbulence could be further considered through the vector component of the airflow.

Funding

This research is funded by the French National Agency for Research in the framework of the PIBE project (contract ANR-18-CE04-0011).

Data availability statement

Data are available on request from the authors.

Conflict of interest

The authors declare that they have no conflicts of interest in relation to this article.

References

1. K. Heutschi, R. Pieren, M. Müller, M. Manyoky, U.W. Hayek, K. Eggenschwiler: Auralization of wind turbine noise: propagation filtering and vegetation noise synthesis. Acta Acustica united with Acustica 100, 1 (2014) 13–24.
2. R. Makarewicz, R. Golebiewski: The partially ensonified zone of wind turbine noise. Journal of Wind Engineering and Industrial Aerodynamics 132 (2014) 49–53.
3. S. Oerlemans, J.G. Schepers: Prediction of wind turbine noise and validation against experiment. International Journal of Aeroacoustics 8, 6 (2009) 555–584.
4. Y. Tian, B. Cotté: Wind turbine noise modeling based on Amiet's theory: effects of wind shear and atmospheric turbulence. Acta Acustica united with Acustica 102, 4 (2016) 626–639.
5. S. Buck, S. Oerlemans, S. Palo: Experimental characterization of turbulent inflow noise on a full-scale wind turbine. Journal of Sound and Vibration 385 (2016) 219–238.
6. T. Van Renterghem, D. Botteldooren: Variability due to short-distance favorable sound propagation and its consequences for immission assessment. Journal of the Acoustical Society of America 143, 6 (2018) 3406.
7. V.E. Ostashev, D.K. Wilson: Statistical characterization of sound propagation over vertical and slanted paths in a turbulent atmosphere. Acta Acustica united with Acustica 104, 4 (2018) 571–585.
8. T. Van Renterghem, K.V. Horoshenkov, J.A. Parry, D.P. Williams: Statistical analysis of sound level predictions in refracting and turbulent atmospheres. Applied Acoustics 185 (2022) 108426.
9. P.D. Nguyen, K.L. Hansen, B. Zajamsek, P. Catcheside, C.H. Hansen: Multi-input model uncertainty analysis for long-range wind farm noise predictions. Applied Acoustics 205 (2023) 109276.
10. B. Cotté: Extended source models for wind turbine noise propagation. Journal of the Acoustical Society of America 145, 3 (2019) 1363–1371.
11. M. West, K. Gilbert, R.A. Sack: A tutorial on the parabolic equation (PE) model used for long range sound propagation in the atmosphere. Applied Acoustics 37, 1 (1992) 31–49.
12. J. Christophe, J. Anthoine, S. Moreau: Amiet's theory in spanwise-varying flow conditions. AIAA Journal 47, 3 (2009) 788–790.
13. B. Kayser, B. Gauvreau, D. Ecotière: Sensitivity analysis of a parabolic equation model to ground impedance and surface roughness for wind turbine noise. Journal of the Acoustical Society of America 146, 5 (2019) 3222–3231.
14. B. Kayser, B. Cotté, D. Ecotière, B. Gauvreau: Environmental parameters sensitivity analysis for the modeling of wind turbine noise in downwind conditions. Journal of the Acoustical Society of America 148, 6 (2020) 3623–3632.
15. T. Foken: Micrometeorology. Springer, 2008.
16. B. Gauvreau: Long-term experimental database for environmental acoustics. Applied Acoustics 74, 7 (2013) 958–967.
17. ISO9613-1:1993: Acoustics Sound attenuation in free field Part 1: atmospheric absorption calculation. Technical report, International Standards Organization, 1993.
18. M.R. Stinson, D.I. Havelock, G.A. Daigle: Simulation of scattering by turbulence into a shadow region using the GF-PE method, in: Sixth International Symposium on Long Range Sound Propagation, Ottawa, Canada, 1994, pp. 283–295. https://apps.dtic.mil/sti/pdfs/ADA290920.pdf#page=296.
19. K. Wert, P. Blanc-Benon, D. Juvé: Effect of turbulence scale resolution on numerical simulation of atmospheric sound propagation, in: 4th AIAA/CEAS Aeroacoustics Conference, Toulouse, France, 2–4 June (1998), p. 2245.
20. B. Gauvreau, M. Bérengier, P. Blanc-Benon, C. Depollier: Traffic noise prediction with the parabolic equation method: Validation of a split-step Pad approach in complex environments. Journal of the Acoustical Society of America 112, 6 (2002) 2680–2687.
21. E.M. Salomons: Computational atmospheric acoustics. Kluwer Academic, The Netherlands, 2001.
22. P. Chevret, P. Blanc-Benon, D. Juvé: A numerical model for sound propagation through a turbulent atmosphere near the ground. Journal of the Acoustical Society of America 100, 6 (1996) 3587–3599.
23. P. Blanc-Benon, L. Dallois, D. Juvé: Long range sound propagation in a turbulent atmosphere within the parabolic approximation. Acta Acustica united with Acustica 87, 6 (2001) 659–669.
24. G.A. Daigle: Effects of atmospheric turbulence on the interference of sound waves above a finite impedance boundary. Journal of the Acoustical Society of America 65, 1 (1979) 45–49.
25. D.K. Wilson, J.G. Brasseur, K.E. Gilbert: Acoustic scattering and the spectrum of atmospheric turbulence. Journal of the Acoustical Society of America 105, 1 (1999) 30–34.
26. D.K. Wilson: A turbulence spectral model for sound propagation in the atmosphere that incorporates shear and buoyancy forcings. Journal of the Acoustical Society of America 108, 5 (2000) 2021–2038.
27. V.E. Ostashev, E.M. Salomons, S.F. Clifford, R.J. Lataitis, D.K. Wilson, P. Blanc-Benon, D. Juvé: Sound propagation in a turbulent atmosphere near the ground: A parabolic equation approach. Journal of the Acoustical Society of America 109, 5 (2001) 1894–1908.
28. Y. Miki: Acoustical properties of porous materials – Modifications of Delany-Bazley models. Journal of the Acoustical Society of Japan 11, 1 (1990) 19–24.
29. H. Müller, C.S. Pedersen: Low-frequency noise from large wind turbines. Journal of the Acoustical Society of America 129, 6 (2011) 3727–3744.
30. R. Kirby: On the modification of Delany and Bazley fomulae. Applied Acoustics 86 (2014) 47–49.
31. D. Ecotière: Influence of turbulence on wind turbine A-weighted SPL prediction, 2022. Available at https://www.umrae.fr/productions/logiciels-applications-et-methodes-de-calcul/windtn/.
32. D. Heimann, Y. Käsler, G. Gross: The wake of a wind turbine and its influence on sound propagation. Meteorologische Zeitschrift 20 (2011) 449–460.
33. E. Barlas, W.J. Zhu, W.Z. Shen, M. Kelly, S.J. Andersen: Effects of wind turbine wake on atmospheric sound propagation. Applied Acoustics 122 (2017) 51–61.

Cite this article as: Kayser B. Écotière D. & Gauvreau B. 2023. Criteria for the assessment of the influence of atmospheric turbulence on wind turbine noise propagation. Acta Acustica, **7**, 63.